NOTE

Environmental Stress Crack Growth in Medium-Density Polyethylene Pipe

Environmental stress cracking (ESC) has been investigated as a tool for evaluating the relative quality of piping materials used for distributing fuel gas. Heretofore unexplained differences in failure times of pipe extruded by different manufacturers from the same medium-density polyethylene resin have been observed. Lot-to-lot variations have also been noted for which no plausible cause could be found. Scanning electron microscopy has revealed that surface features of the pipe can contribute to premature failure in polyethylene piping material.

EXPERIMENTAL

Two lots of 1-in.-diam (2.54 cm) polyethylene pipe corresponding to ASTM designation PE 2306,[1] both made from the same material but processed by different extruders, were tested in the compressed-ring constant strain test. The test was first described by Rader[2] and is being balloted by ASTM for possible adoption as a recommended procedure. In effect, the test approximates the stress configuration in the more common bent strip test developed by Bell Laboratories.[3]

The compressed-ring method (for 1-in. pipe) consists of cutting a 12.7-mm-wide ring out of the pipe and pressing a razor blade 0.64 mm deep into the outside wall at the center of the ring, parallel to the edge. The notch is 19 mm long and is consistently located in the region of minimum wall thickness.

Eight of these specimens are mounted between two compression plates with the notched area positioned parallel to the direction of compression. The specimens are compressed so that the plates are 9.14 mm apart and are then placed in a 25% solution of the stress cracking agent at 50°C. The times for crack initiation are recorded. A picture of the compressed ring fixture with specimens prior to immersion in Igepal are shown in Figure 1.

The stress cracking agent used in this test, Igepal CO-630 (GAF Corp.), is a highly polar, nonionic surfactant with the following structure:

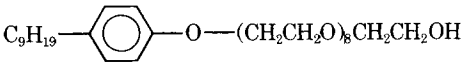

Samples were removed from the solution at different times prior to complete fracture, washed, air dried, and axially cut in half so the uncracked portion could be discarded. The cracked half was subsequently coated with gold by vacuum deposition while under the same degree of bending as in the test, and was then observed while bent in the scanning electron microscope (SEM).

RESULTS

Average failure times for the two lots of materials processed by different extruders varied by an order of magnitude although the compound was purportedly the same. The average failure time for lot 1 was 237 hr, while that for lot 2 was 24 hr. This anomaly was even more puzzling because the two materials, after extrusion, did not differ appreciably in average molecular weight, molecular weight distribution, or density (Table I). A tendency noted in the lot exhibiting better resistance was that cracks originated solely in the razor notch region. The poorer lot exhibited failures which usually started on the unnotched side of the specimen, with failures on the notched side taking place at a later time.

Figure 2 shows a typical failure for lot 1 material in the SEM, with the insert showing a photograph of the same specimen. The razor notch is shown in the vertical direction. The crack wall displays a wavelike pattern distributed radially around the notch which indicates crack initiation at this point. At A a crack just starting at the notch is shown. This is also shown in Figure 3 at higher magnification.

Journal of Applied Polymer Science, Vol. 26, 1049–1056 (1981)
 CCC 0021-8995/81/031049-07$01.00

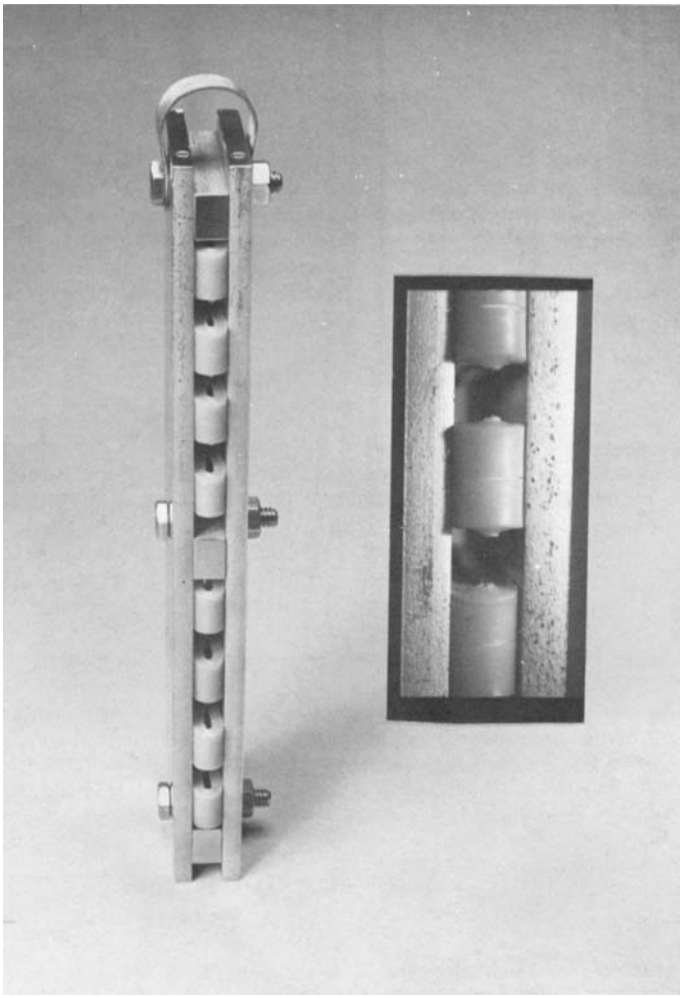

Fig. 1. Photograph of pipe specimens in the compressed-ring fixture prior to immersion in Igepal.

Because the crack started at a point below the surface, the crack front is an arc which moves radially from that point. Therefore, the crack propagation undercuts the surface as seen at B in Figure 3, where the surface is just beginning to part. More evidence that the crack propagated from the lower notch area can be derived from the wave-like pattern on the fracture surface in Figure 2. This pattern can be interpreted as earlier crack fronts for the advanced stress crack shown. Because the crack grows radially from the root of the notch, the portion of the crack on the same depth as the notch root is further from the notch than the portion of the crack which appears on the specimen surface. Similar notch initiation and subsurface cracking has been documented previously.[4]

Figure 4 shows a lot 2 failure on the notched side of the specimen. The crack appears more irregular in contrast to the symmetry of the crack around the notch in the lot 1 sample. The large crack on the right of Figure 4 appears to have grown independently of the notch.

At higher magnification (Fig. 5), this large crack is seen surrounded by a number of superficial cracks, a few of which are shown at C, D, and E. These small cracks seem to be initiated directly from the surface voids that are readily evident at this magnification and can be seen over the entire specimen surface. Presumably, the large crack in the center of the figure also originated from one of these voids and would connect with the crack to its left if the specimen had remained in the Igepal.

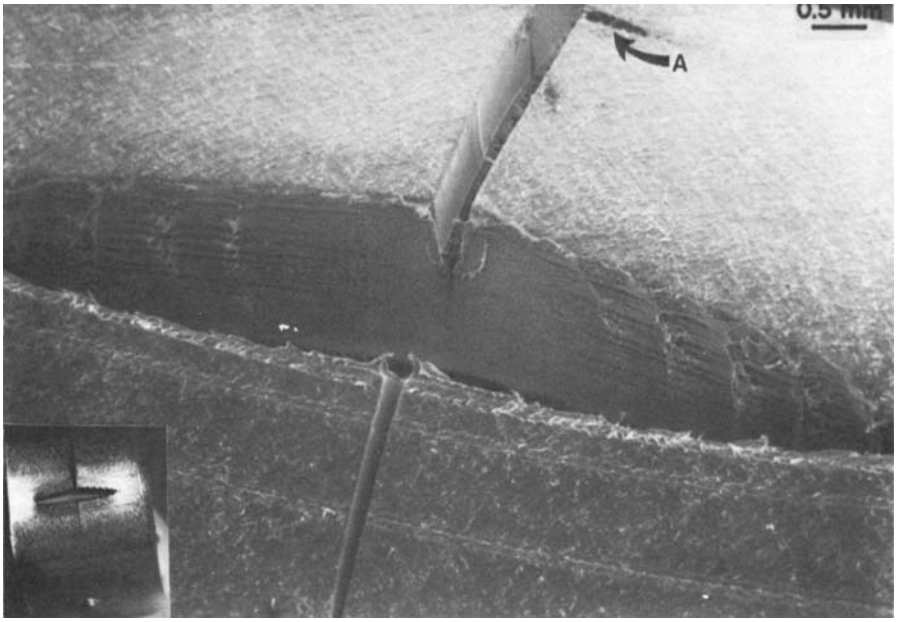

Fig. 2. SEM micrograph of notched portion of lot 1 compressed-ring specimen removed from the Igepal bath during crack formation (vertical groove is the razor notch.) A denotes small crack initiating at the notch. Insert: photograph of the same specimen.

Evidence of a similar cracking mode can be seen on the left side of the notch (Fig. 6) with the characteristic superficial cracks being shown at F and G. More proof of surface-initiated crack growth can be seen at H, where another crack seems to have propagated radially from a point on the surface of the specimen. However, evidence of notch initiation can also be seen at N in Figure 5, showing radial crack propagation from the notch root on the fracture surface.

Figure 7 shows a lot 2 failure on the unnotched side of the specimen, an indication again of surface initiated failure. Crack formation on the unnotched side of the specimen appeared far earlier than cracks on the notched side for lot 2 material. The crack on the left side of the specimen is shown at higher magnification in Figure 8. This crack clearly shows an advancing crack front propagating radially from the surface. The crack on the right side of the same specimen, shown in Figure 9, seems to consist of two advancing cracks which have connected at the ridge shown at I. This ridge, which is the remnant of the material between the growing cracks, displays longer fibers in contrast to the short fibers on the remainder of the fracture surface. Evidently, this morphology occurred through a combination of environmental stress cracking and ductile failure, the latter occurring because the cross section of the interface became thinner and could not support the load presented by the bending stress. These longer fibers, which are shown at higher magnification in Figure 10, appear "corrugated." This appearance has been observed previously by other workers[5] and has been explained as the effect of the retraction of fibers after they were drawn out.

TABLE I
Properties of Lot 1 and Lot 2 Medium-Density Polyethylene (PE2306) Piping Materials

Property	Lot 1	Lot 2
Weight-average molecular weight M_w	127,900	128,500
Number-average molecular weight M_n	15,300	14,500
Polydispersity index M_w/M_n	8.4	8.9
Z-average molecular weight		
M_z	884,400	864,300
$M_z + 1$	2,274,400	2,395,200
Density, g/cm^3 ρ	0.9403	0.9383

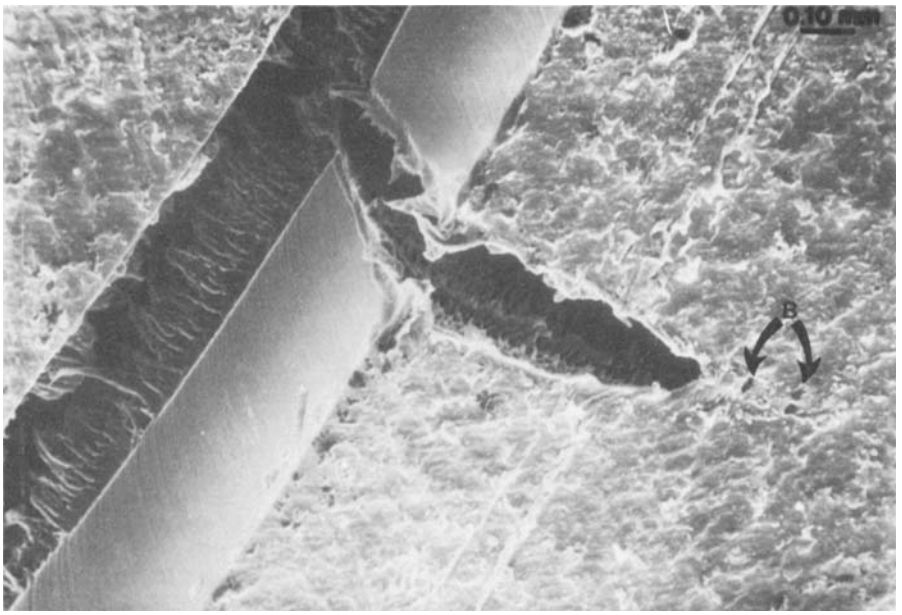

Fig. 3. SEM micrograph of notched portion of lot 1 compressed-ring specimen removed from the Igepal bath during crack formation. Area A in Fig. 1 shown at higher magnification. Crack propagation undercutting the specimen surface is shown at B.

DISCUSSION

Two major theories have been advanced to explain environmental stress cracking. Hopkins, Baker, and Howard[6] theorized that the stress cracking agent exerts a spreading pressure in intrinsic flaws and cracks on the polymer surface. Spreading pressure, in conjunction with applied mechanical

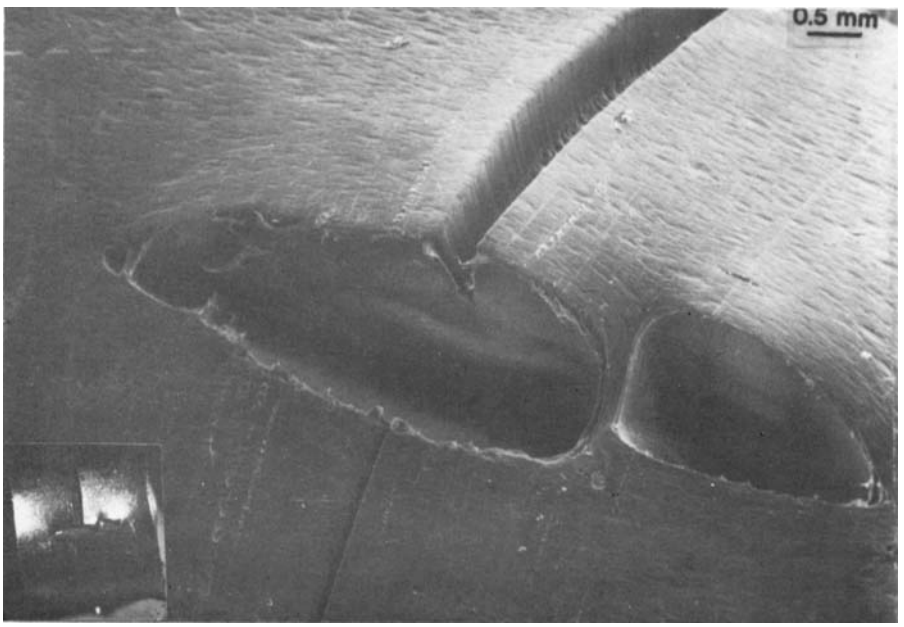

Fig. 4. SEM micrograph of notched portion of lot 2 compressed-ring specimen removed from the Igepal bath during crack formation. Insert: photograph of the same specimen.

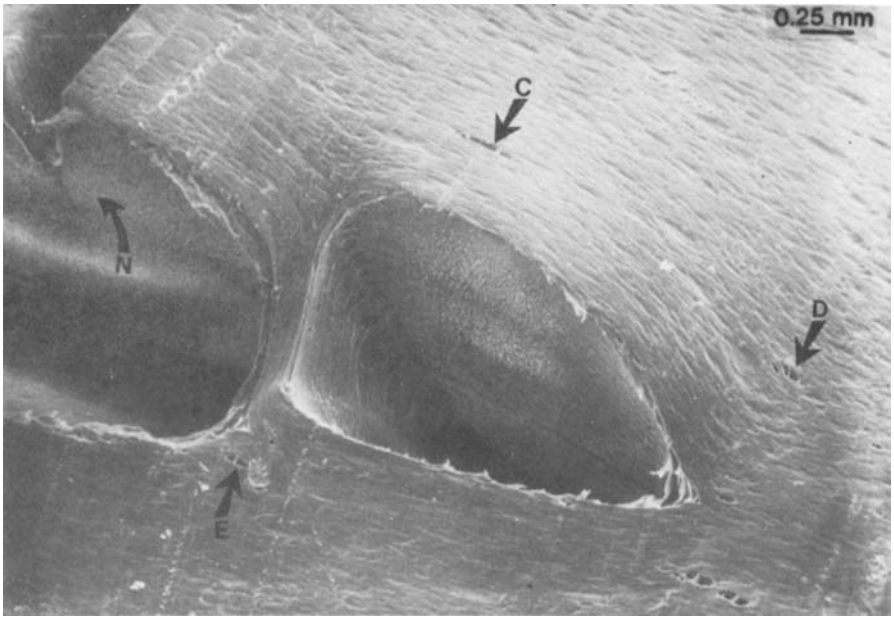

Fig. 5. SEM micrograph of notched portion of lot 2 compressed-ring specimen removed from the Igepal bath during crack formation. Right crack in Fig. 3 is shown at higher magnification. Superficial cracks are shown at C, D, and E.

stress, results in crack initiation. On the other hand, Isaksen, Newman, and Clark[7] ascribed the role of the stress cracking agent to interference with the uniform formation of fibers which takes place after spherulitic collapse upon drawing. Subsequent publications seemed to display a preference for the latter theory. For example, Frayer, Tong, and Dreher[8] explain ESC as the relaxation

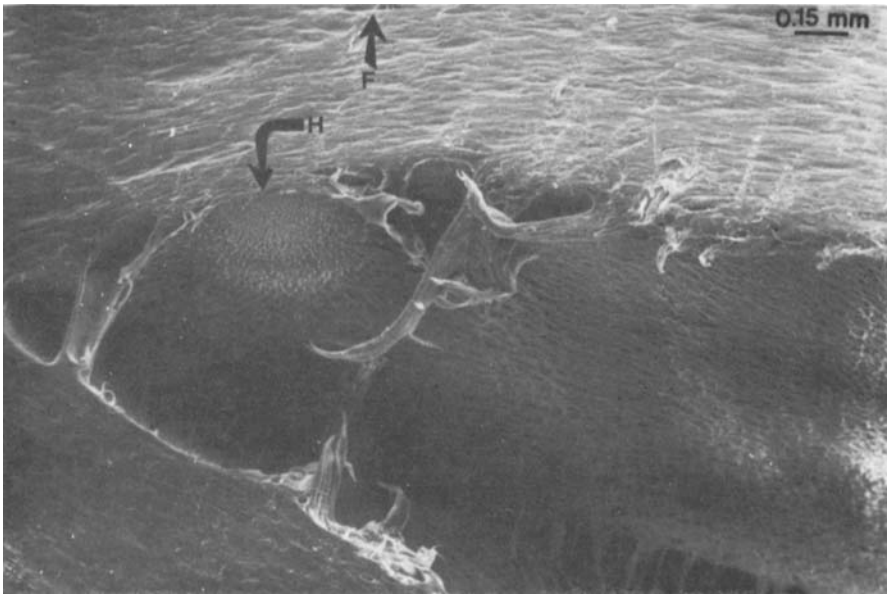

Fig. 6. SEM micrograph of notched portion of lot 2 compressed-ring specimen removed from the Igepal bath during crack formation. Left portion of crack in Fig. 3 shown at higher magnification. Superficial cracks are shown at F and G. Evidence of surface initiation is shown at H.

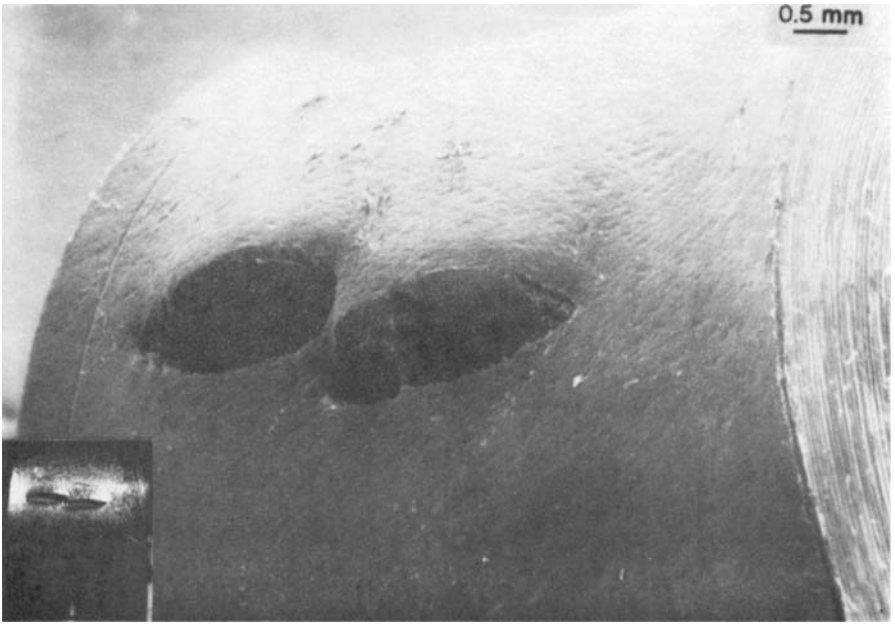

Fig. 7. SEM micrograph of unnotched portion of lot 2 compressed-ring specimen removed from the Igepal bath during crack formation. Insert: photograph of the same specimen.

of tie molecules, which must of course remain stiff for uniform fiber deformation to take place. Singleton, Roche, and Geil[5] found that in thin films under tension in ESC agents, small blocks of lamellae remained undrawn. Toggenburger and Newman[9] found that polyethylene is most vulnerable to ESC when stressed just short of yield, i.e., where spherulites are just being transformed to microfibrils.

Although the theory of Isaksen et al.[7] is now widely accepted as the most plausible ESC mechanism,

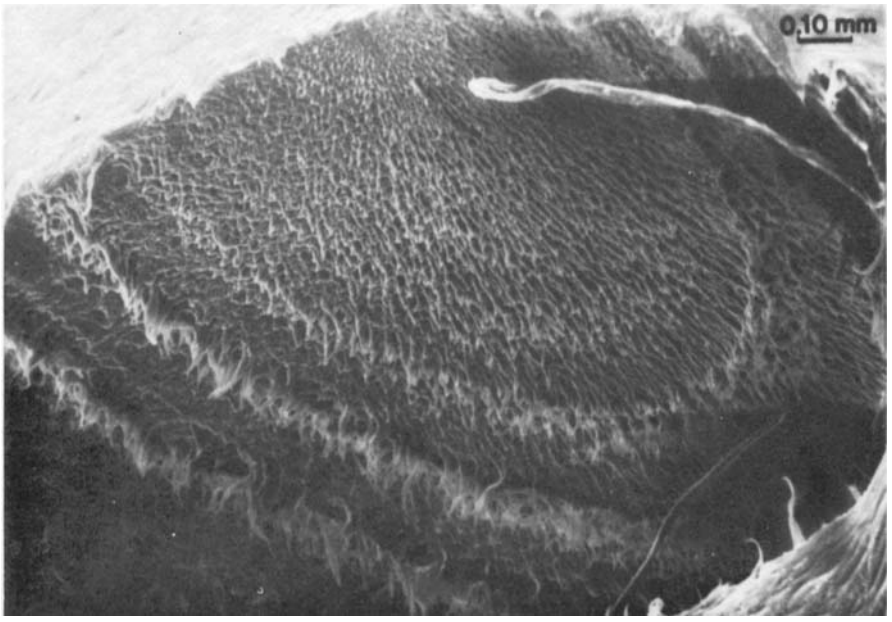

Fig. 8. SEM micrograph of unnotched portion of lot 2 compressed-ring specimen removed from the Igepal bath during crack formation. Left crack in Fig. 7 is shown at higher magnification.

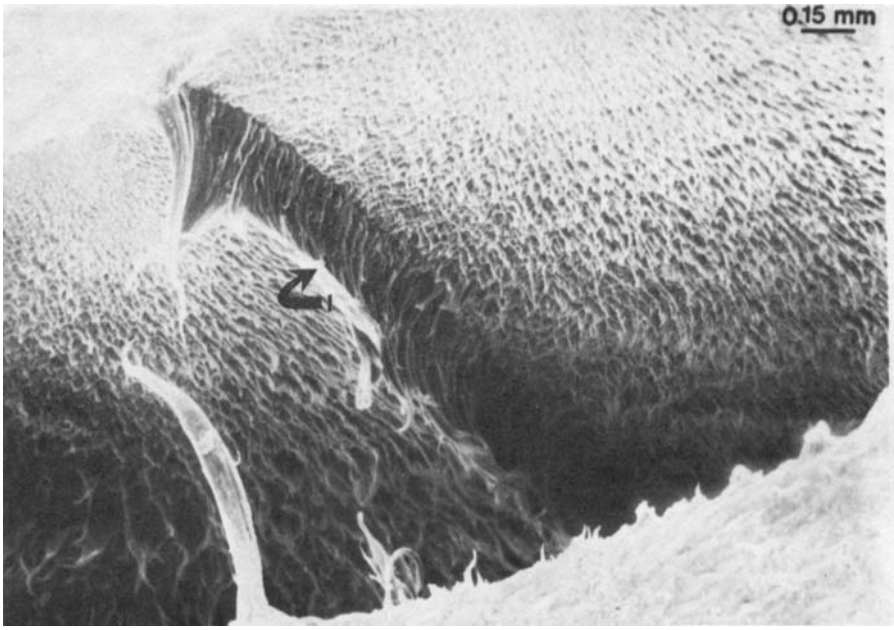

Fig. 9. SEM micrograph of unnotched portion of lot 2 compressed-ring specimen removed from the Igepal bath during crack formation. Right crack in Fig. 7 is shown at higher magnification.

present test results indicate that the influence of flaws on the polymer surface cannot be discounted. Even though, on a molecular level, the interference to uniform fiber formation is the ultimate cause of failure, voids on the specimen surface greatly accelerate this effect, probably through stress concentrations. It was found that failures in the lot 2 materials typically occurred on the unnotched side of the specimen because the notch on the other side of the specimen relieved stresses in the bending direction and retarded cracking. Thus, the biaxial stress condition effected by the notch, which is so important for ESC to occur in low-density and most medium-density polyethylenes,[10] actually prolongs time to failure in this case.

Surface roughness per se seems to have no accelerating effect on ESC as can be discerned from the relatively rough surface of the highly ESC-resistant lot 1 material. Cracks on the specimen surfaces seem to originate only at voids. The evidence here may indicate that before the voids actually develop into cracks, crazed material forms in the interim since the small superficial cracks appear to be bridged by intervening fibers at C, D, E, F, and G in Figures 4 and 5. Crazing as the precursor to environmental stress cracking has been shown for high-density polyethylene.[11,12]

The voids evident in the lot 2 samples seem to be oriented parallel to the specimen width or parallel to the extrusion direction. These voids may have formed as a result of a very rapid quench after the extrusion process which would cause widespread local shrinking due to precipitous crystallization on the surface.

CONCLUSIONS

Environmental stress cracks in notched samples of medium-density polyethylene pipes were found to originate either at the notch or on the specimen surface, depending on the morphology of that surface. The samples which displayed surface initiated failures correspondingly showed a much shorter failure time than the specimens in which the failure originated in the notch, even though material parameters such as average molecular weight, molecular weight distribution, and density were similar. In addition, samples showing surface-initiated cracking typically failed on the unnotched side of the specimen. The origin of surface-initiated failure can be traced to voids aligned in the extrusion direction on the specimen surface. These voids are a source of stress concentrations on the specimen, and, as a result, cracks are initiated on the surface.

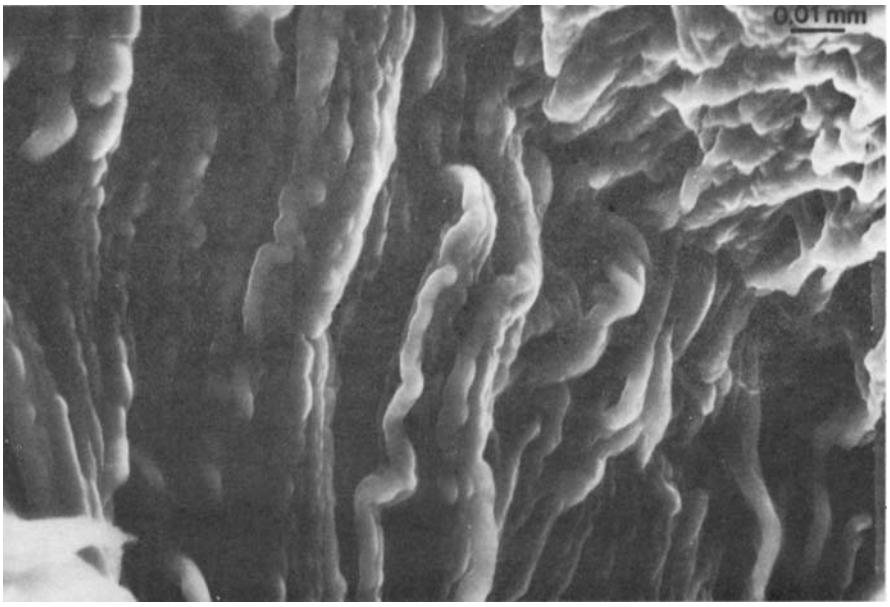

Fig. 10. SEM micrograph of unnotched portion of lot 2 compressed-ring specimen removed from the Igepal bath during crack formation. I region of Fig. 9 is shown in higher magnification.

The authors wish to thank the Gas Research Institute, under whose sponsorship this work was performed. The collaboration of Michael J. Cassady for the ESCR setup, Andrew Skidmore for his help on the SEM, and the rest of our colleagues at Battelle is also appreciated. Gas Research Institute makes no warranty as to the accuracy or completeness of this report and assumes no liability for the use of information disclosed in this article.

References

1. ASTM Standard D3350-78, *1980 Book of ASTM Standards*, Part 34.
2. A. M. Rader, Fifth A. G. A. Plastic Pipe Symposium, Houston, TX, Nov. 13–15, 1974.
3. ASTM Standard D1693-70, *1980 Book of ASTM Standards*, Part 36.
4. A. Lustiger, R. D. Corneliussen, and M. R. Kantz, *Mater. Sci. Eng.*, **33**, 117 (1978).
5. C. J. Singleton, E. Roche, and P. H. Geil, *J. Appl. Polym. Sci.*, **21**, 2319 (1977).
6. I. L. Hopkins, W. D. Baker, and J. B. Howard, *J. Appl. Phys.*, **21**, 207 (1950).
7. R. A. Isaksen, S. Newman, and R. J. Clark, *J. Appl. Polym. Sci.*, **7**, 515 (1963).
8. P. D. Frayer, P. P. Tong, and W. W. Dreher, *Polym. Eng. Sci.*, **7**, 27 (1977).
9. R. Toggenburger and S. Newman, *J. Polym. Sci. Part B*, **2**, 7 (1964).
10. J. B. Howard, in *Crystalline Olefin Polymers*, Part II, R. A. V. Raff and K. W. Doak, eds., Wiley–Interscience, New York, 1964, p. 47.
11. A. Lustiger and R. D. Corneliussen, *J. Polym. Sci. Part B*, **17**, 269 (1979).
12. S. Bandyopadhyay and H. R. Brown, *Polym. Eng. Sci.*, **20**, 720 (1980).

A. LUSTIGER
R. L. MARKHAM
M. M. EPSTEIN

Battelle
Columbus Laboratories
Columbus, Ohio 43201

Received June 9, 1980
Accepted September 18, 1980